Indian Journal of Chemistry
Vol. 58A, April 2019, pp. 436-445

Spectro-analytical and *in vitro* biological studies of novel nalidixic acid hydrazone and its transition metal complexes

Nagula Narsimha, Mohmed Jaheer, Palreddy Ranjith Reddy, Kunche Sudeepa & Ch. Sarala Devi*

Department of Chemistry, University College of Science, Osmania University, Hyderabad, Telangana, India

Email: dr_saraladevich@yahoo.com

Received 25 May 2018; revised and accepted 5 March 2019

The novel and potential chelating agent derived from Nalidixic acid and its binary Cu(II), Ni(II) and Co(II) metal complexes have been synthesized and characterized by elemental analyses, ^{1}H-NMR, Mass, UV-vis, FT-IR, TGA, SEM-EDX, ESR and magnetic susceptibility measurements. All the systems of the present study have been screened for antimicrobial activity against bacterial species *Bacillus* (Gram +) and *Escherichia coli* (Gram –) and fungal species *Sclerotium rolfsii* and *Macrophomina phaseolina* exhibited an enhanced activity of metal complexes over unbound free chelating agent. The interaction studies of metal complexes with Calf-thymus DNA (CT-DNA) investigated by UV-visible and fluorescence titrations revealed the intercalation mode of binding. Further MTT assay performed on HeLa (human cervical cancer) and A549 (human lung tumor) cell lines revealed the IC_{50} values for the studied title compounds. In addition computer-aided molecular docking technique carried out with all title compounds employing molecular target DNA (PDB ID: 1N37), furnished docking scores and mode of binding for geometry optimized molecular structures of title compounds.

Keywords: Nalidixic acid, Antimicrobial activity, DNA interactions, MTT assay, Molecular docking

Hydrazones and their transition metal complexes have attained much importance in inorganic and medicinal chemistry in view of their diverse biological and pharmacological activities[1]. In general the role of transition metal complexes has been found to be essential to reveal the complexity in biology[2]. The interaction of transition metal complexes with DNA has been extensively studied in the past few years due to their possible applications in molecular biology and cancer therapy[3-11]. DNA being the primary target molecule for most antiviral and anticancer therapies, the binding mode of interaction between a novel transition metal complex and DNA has been a subject of basic research in bioinorganic chemistry in recent years[12-15]. Basically, metal complexes bind to DNA double helix via non-covalent modes including intercalative, external electrostatic and groove binding[16-19] or covalent modes, a proper understanding of which, could be critical for explaining DNA. Among them the intercalative binding mode is significantly important as it results in the formation of more stable DNA-metal complex adduct. Molecular recognition has a central role in rational drug design[20]. Binding affinity and interactions are two key components which aid to understand the molecular recognition in drug-receptor complex and are crucial for structure-based drug design in medicinal chemistry[21]. The choice of metal ion is the most significant factor in the design of metal based chemotherapeutic agents[22]. There has been growing interest in the investigation of Cu(II), Co(II) and Ni(II) metal complexes for their interaction with DNA[23-28] as is evident from literature[29-35]. Such complexes exhibit antibacterial, antifungal, anti-cancer and cancer inhibiting properties.

In the present investigation, some transition metal complexes of novel Nalidixic acid hydrazone were synthesized keeping in view the significant biological activity of its precursor nalidixic acid and its metal complexes reported earlier[36]. The spectroscopic characterization of synthesized novel nalidixic acid hydrazone; [N'-(2-hydroxy-5-nitrobenzylidene)-1-ethyle-1,4-dihydro-7-methyle-4-oxo-18-naphthyridine -3-carbohydrazone (NTEMNC)] and its solid Cu(II), Ni(II) and Co(II) metal complexes and the evaluation of their antimicrobial activity, DNA interaction, cytotoxicity and docking studies have been reported herein.

Materials and Methods

Calf-thymus DNA (CT-DNA) (50 μg/test) was purchased from Bangalore genei. HeLa (Cervical

cancer cell line) and A549 (human lung tumor cell line) were purchased from NCCS, Pune. MTT [3-(4, 5-dimethylthiazol-2-yl)-2, 5-diphenyltetrazolium bromide], DMEM (Dulbecco's modified Eagles medium), EDTA and Phosphate Buffered Saline (PBS) were purchased from Sigma Chemicals and Fetal Bovine Serum (FBS) was purchased from Gibco. Nalidixic acid and all other chemicals were purchased from Sigma Aldrich.

UV-Visible spectra were recorded with a Shimadzu UV-2600 Spectrophotometer. Fluorescence measurements were performed on a JASCO FP-8500 Spectrofluorimeter. The IR spectra were recorded on KBr disks on Shimadzu IR Prestige-21 Spectrophotometer. ^{1}H-NMR spectra were recorded on a Bruker WH (400 MHz) Spectrometer with $CDCl_3$ as solvent. Thermal analyses were carried out using Shimadzu TGA-50H in nitrogen atmosphere; SEM images were recorded in INCA EDX analyzer. The elemental analyses of compounds under study were carried out on atomic absorption spectrophotometer (ELICO-SL 163). ESI-MS mass spectra were recorded on VG AUTOSPEC mass spectrometer. Magnetic properties of metal complexes have been determined on a Gouy balance model 7550 at room temperature using Hg $[Co(SCN)_4]$ as standard. ESR spectra were scanned on JES - FA200 ESR Spectrometer with X band at 77 K (liquid nitrogen temperature). Melting points were determined in Polmon apparatus (model no. MP-90).

Synthesis of nalidixic acid hydrazone [N'-((2-hydroxy-5-nitrobenzylidene)-1-ethyl-1, 4-dihydro-7-methyl-4-oxo-1, 8-naphthyridine-3-carbohydrazide (NTEMNC)] involves three steps[37].

Step-I: Synthesis of nalidixic acid ester: Nalidixic acid (3 g) and tetrahydrofuran (100 mL) were taken in a 250 mL round bottom flask and mounted over a magnetic stirrer. Anhydrous potassium carbonate (8.96 g) was added and the contents were stirred for 1 h. Dimethyl sulfate (2.475 mL) was added to this stirred solution and the mixture was refluxed at 60–80 °C. The progress of the reaction was monitored by TLC using hexane/ethyl acetate (70:30) as the eluent. After 6 h, a new spot was observed on the TLC plate. After the completion of reaction, the solvent was removed under reduced pressure using a rotary evaporator and the product was extracted with chloroform. The chloroform layer was dried over anhydrous sodium sulfate and concentrated under reduced pressure to give the desired ester.

Step-II: Synthesis of nalidixic acid hydrazide: The above synthesized ester (2 g) was dissolved in tetrahydrofuran (60 mL) in a 250 mL round bottom flask and hydrazine hydrate ($NH_2NH_2.H_2O$, 0.8 mL) was added. The contents were refluxed for 3 h. To the resultant reaction mixture, cold water (100 mL) was added and the mixture stirred for 30 min. The separated solid was filtered using a pump and dried.

Step-III: Synthesis of nalidixic acid hydrazone (NTEMNC): The above prepared hydrazide (0.1 mol) and 2-hydroxy-5-nitrobenzaldehyde (0.1 mol) were dissolved in methanol (50 mL). The mixture was refluxed at 60–70 °C on a magnetic stirrer for 2–3 h. The progress of the reaction was monitored by TLC. After completion of the reaction, the product was cooled to room temperature. The solid obtained was filtered and washed with methanol and recrystallized from aqueous ethanol to obtain pure compound (m.pt 310 °C) (Scheme 1). The metal complexes were prepared by refluxing the solution of hydrazone (NTEMNC) dissolved in chloroform and corresponding $Cu(II)Cl_2.6H_2O$, $Ni(II)Cl_2.6H_2O$ and $Co(II)Cl_2.6H_2O$ metal salts in ethanol (1:2 mol) for 15–18 h at 60–80 °C and by adjusting pH in the range 6.5–7.5 for complex formation. The resulting solutions were concentrated and cooled. On cooling, the colored metal complexes obtained were filtered and washed several times with ethanol and chloroform. These were then dried and stored in desiccators over anhydrous $CaCl_2$.

In the present investigation AutoDock 4.2 software[38] was employed to carry out molecular docking studies of the synthesized hydrazone and its metal complexes with the DNA target. In order to carry out molecular docking with DNA, crystal structure of double stranded DNA molecule $(AGACGTCT)_2$ (PDB ID: 1N37) was downloaded from protein data bank (www.rcsb.org)[39]. It was prepared by protein preparation wizard applying OPLS 2005 force field in Schrödinger suite. A grid was prepared around the intercalation site by selecting the co-crystallized ligand. Metal complexes were constructed and optimized in ChemDraw. These were docked into DNA intercalation site and molecular interaction diagrams were obtained from PMV (Python Molecular Viewer) [40].

Absorption studies were recorded on a Shimadzu160A UV-visible spectrophotometer. Absorption titration experiments were performed with a fixed concentration of metal complex (5 μM) and by

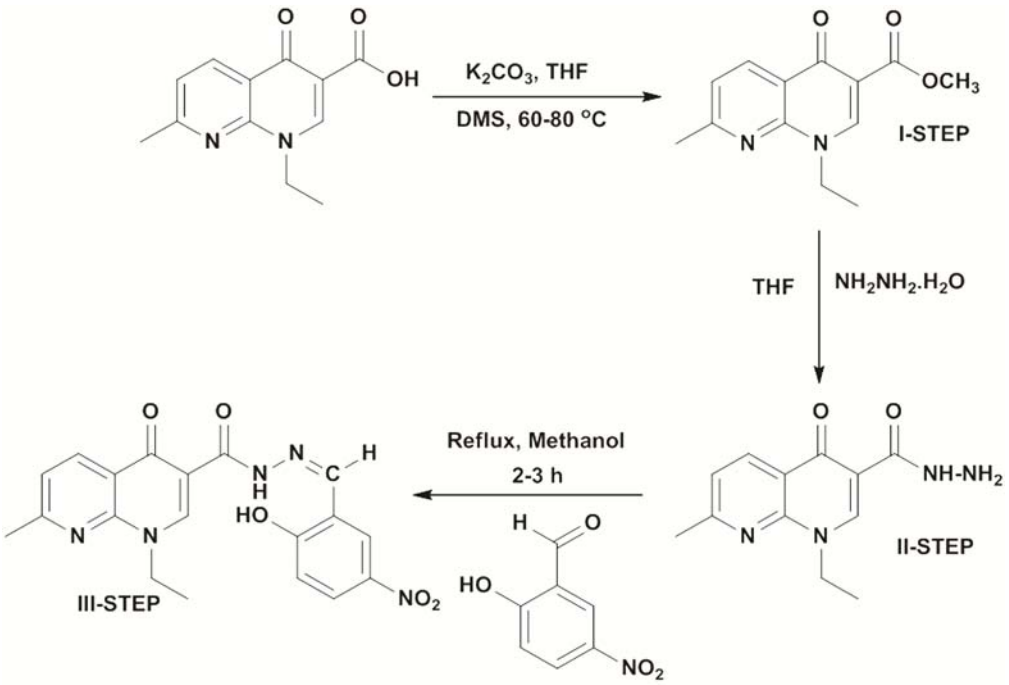

Synthetic path for NTEMNC

Scheme 1

varying the concentration of CT-DNA (0–5 μM) according to the reported procedure[41]. The titration was continued until there was no change in absorbance which indicates the saturation point for binding. For the complexes Cu(II), Ni(II) and Co(II), the binding constants (K_b), were determined from the spectroscopic titration data using the following equation:

$$[DNA]/ (\varepsilon_a - \varepsilon_f) = [DNA]/ (\varepsilon_b - \varepsilon_f) + 1/K_b (\varepsilon_b - \varepsilon_f) \ldots (1)$$

The apparent absorption coefficient ε_a, corresponds to A_{obs}/[metal complex] in the absence of DNA. In presence of DNA, the terms ε_f and ε_b correspond to the extinction coefficient of the free metal complex (unbound) and the fully bound metal complex to DNA respectively[42].

The binding of metal complexes to CT-DNA was also studied by fluorescence technique. Fluorescence study was performed on a JASCO FP-8500 spectrofluorimeter. The change in fluorescence intensity at 605 nm was recorded by adding the solution of metal complex in small increments, to the mixture of ethidium bromide (EB) (36 μM) and DNA (36 μM).

The fluorescence quenching is described by the Stern-Volmer relation[43]:

$$I_0/I = K_{sv} [r] + 1 \quad \ldots (2)$$

where I_0 and I represent the fluorescence intensities in the absence and presence of the quencher, respectively. K_{sv} is a linear Stern-Volmer quenching constant, and [r] is the quencher concentration. The quenching constant (K_{sv}) can be obtained using the plot of log (I_0/I) versus [r].

For a static quenching interaction, the fluorescence intensity data can also be used to determine the apparent binding constant (K_q) and the number of binding sites (n) for the complex by the following equation[44]:

$$\log [F_0 - F/ F] = \log K_b + n \log [Q] \quad \ldots (3)$$

From the plot of log [(F_0 − F/F)] versus log [Q], the binding stoichiometry (n) has been obtained from the slope and binding constant (K_b) from intercept value.

The synthesized hydrazone and its Cu(II), Ni(II) and Co(II) complexes with different concentrations (25, 50 and 100 μM) were screened for the *in vitro* antibacterial activity with Gram-positive bacteria (Bacillus) and Gram-negative bacteria (*Escherichia coli*) and antifungal activity against two fungi species (*Macrophomina phaseolina* and *Sclerotium rolfsii*) by using standard procedure[45].

The *in vitro* anticancer activity was measured using the 3-(4,5-dimethylthiazol-2-y1)-2,5-diphenyltetrazolium bromide (MTT) assay[46]. HeLa (human cervical cancer cell line) and A549 (human

lung tumor cell line) were maintained in Dulbecco's Modified Eagle's medium (DMEM), supplemented with 10% Fetal Bovine Serum (FBS) and the antibiotics penicillin/streptomycin (0.5 mL^{-1}), in an atmosphere of 5% CO_2/ 95% air at 37 °C. Cell viability was evaluated by the MTT assay with three independent experiments with 10, 25, 50, 75 and 100 µM concentration of compounds in triplicates. Cells are trypsinized and the trypan blue assay is performed to know viable cells in cell suspension. Cells are counted by haemocytometer and seeded at a density of 5.0×10^3 cells /well in 100 µL media in 96 well plate culture medium and incubated overnight at 37 °C. After incubation, the old medium is removed and 100 µL of fresh medium and different concentrations of the test compound are added into representative wells of 96 plates, and then incubated for 48 h. After 48 h, the MTT solution (0.5 mg/mL) was added to each well and plates were incubated at 37 °C for 3 h. At the end of incubation time, the precipitate forms as a result of reduction of MTT salt to chromophore formazan crystals by the cells with metabolically active mitochondria. The optical density of solubilized crystals in DMSO was measured at 570 nm on a microplate reader. The percentage growth inhibition was calculated and concentration of test drug needed to inhibit cell growth by 50% values was generated from the dose-response curves for each cell line using linear regression equation[47].

Results and Discussion

Spectral studies of NTEMNC

Mass and elemental analyses

The mass spectrum of ligand (NTEMNC) displayed (Supplementary Data, Fig. S1) a peak at *m/z* 395, that corresponds to the molecular ion peak. Elemental analyses (Found: C 57.70; H 4.10; N 17.90; Calcd: C 57.72; H 4.03; N 17.71 %) indicated the composition of title compound as $C_{19}H_{17}N_5O_5$.

^{1}H- NMR

The ^{1}H-NMR spectrum of NTEMNC showed (Fig. S2) a signal at δ 13.40 ppm corresponding to amide proton (s, NH). The signal at δ 10.01 ppm is (s, -CH=N-) attributed to azomethine proton and the peak at δ 11.60 ppm (s, OH) to phenolic OH which is further identified with D_2O exchange spectrum (Fig. S3). The other signals were recorded at δ 8.68 ppm (s, 1H, H-2-napthyridine), δ 8.98 ppm (d, 1H, H-5-napthyridine), δ 8.42 ppm (d, 1H, H-6-napthyridine), δ 7.07–8.18 ppm (m, 3H, aromatic), δ 4.60 ppm (q, 2H, N-CH_2), δ 1.56 ppm (t, 3H, N-CH_2 $\underline{CH_3}$), and δ 2.71 ppm (s, 3H, 7-$\underline{CH_3}$).

Infrared spectral studies

IR spectrum of NTEMNC showed the presence of a broad band centered at (Fig. S4) 3493 cm^{-1} attributed to phenolic ν (OH) and amide ν (N-H) group stretching vibrations. The small intense bands noticed at 3039 cm^{-1} and 2983 cm^{-1} are due to aromatic ν (C-H) and aliphatic ν (C-H) stretching vibrations. The strong intense bands at 1612 cm^{-1} and 1680 cm^{-1} correspond to the quinolone ring ν (C=O) stretching vibrations. The spectrum also showed bands at 1570 cm^{-1} , 1292 cm^{-1} and 1340 cm^{-1} corresponding to azomethine ν (C=N), phenolic ν (C-O) and ν (N=O) stretching vibrations respectively.

UV-Visible spectral studies

The spectrum showed (Fig. S5) three bands at 267 nm (37453.18 cm^{-1}), 292 nm (34246.58cm^{-1}) and 323 nm (30959.75 cm^{-1}) corresponding to the n→ π* transition of the C=O and n→ π* transitions of the C=N group.

Characterization of metal complexes

The metal complexes of the present investigation were characterized with the data obtained from various analytical and spectral techniques viz., elemental analyses, mass, IR, UV-vis, TGA, SEM, EDX, ESR and measurement of magnetic susceptibilities.

All the metal complexes are colored, amorphous in nature and soluble in DMSO. Conductivity measurements made in DMSO medium, indicated their non-electrolytic nature.

Mass and elemental analyses

The mass spectral peaks displayed (Fig. S6, S7 and S8) at *m/z* 851, 846 and 847 in Cu(II), Ni(II) and Co(II) complexes respectively and the results obtained from elemental analyses presented in Table 1, showed metal to ligand ratio as 1:2 (M:2L) in all the aforementioned complexes.

Infrared spectral studies

The IR spectra provided valuable information about the type of donor sites attached to the metal ion in a complex. The IR spectrum of the ligand is compared with the IR spectra of its Cu(II), Ni(II) and Co(II) metal complexes (Fig. S9). All the metal complexes showed a new broad band in the region 3400–3592 cm^{-1} which can be attributed to ν (OH) of coordinated water molecules[48] and two weaker bands in the region 820–840 cm^{-1} and 710–760 cm^{-1} [49] due to rocking and wagging modes of vibrations. The

–CH=N stretching frequency in the IR spectrum of ligand observed at 1570 cm^{-1} is shifted towards lower frequency (1544, 1527 and 1530 cm^{-1}) in Cu(II), Ni(II) and Co(II) metal complexes respectively indicating the participation of (–CH=N) nitrogen (N) in coordination with the metal (II) ion with the donation of lone pair of electrons having slight bonding character [50]. The phenolic ν (C-O) band is shifted from 1292 cm^{-1} to the region of 1230–1247 cm^{-1} [51] in all metal complexes, indicating the participation of phenolic oxygen (O) in metal-oxygen bond formation. In addition, new bands around 430–475 cm^{-1} and 550–596 cm^{-1} in all complexes, correspond to ν (M-N) and ν (M-O) [52] respectively.

Electronic spectral studies

The electronic spectrum of free ligand (NTEMNC) and its metal (II) complexes were recorded in DMSO solution (10^{-3} M) in the range of 200–800 nm. The complexes exhibited (Fig. 1) distinct electronic transitions, which may be attributed to spin and vibronically allowed *d-d* transitions under respective stereochemistries, wherein Cu(II) complex displayed bands at 700 nm (14285.71 cm^{-1}), 472 nm (21186.44 cm^{-1}) and 405 nm (24691.36 cm^{-1}), Ni(II) complex at 701 nm (14265.34 cm^{-1}) and 447 nm (22371 cm^{-1}), and, Co(II) complex at 703 nm (14224.75 cm^{-1}) and 400 nm (25000 cm^{-1}) .

SEM and EDX studies

The SEM images of ligand and its Cu(II), Ni(II) and Co(II) complexes displayed (Fig. S10–S13) distinct morphology. The EDX analyses of all metal complexes revealed the elemental composition wherein absence of chlorine is evident, thus confirming the binding of metal ion with mono-ionized form of ligand in 1:2 ratio ($M:L_2$) by the displacement of two chloride ions from metal salt.

Thermal studies

Thermogravimetric analysis (TGA) is a useful technique in evaluating the thermal stability of the metal complexes. The thermal analyses of Cu(II), Co(II) and Ni(II) complexes were carried out at a heating rate of 10 °C min^{-1} under nitrogen atmosphere. Thermograms of Cu(II), Co(II) and Ni(II) complexes are given in Fig. 2. The results obtained suggested that all metal complexes exhibit distinct decomposition process mainly in three stages. The first stage of decomposition in the range of 120–210 °C corresponds to the loss of two coordinated water molecules. In the second step, a sudden weight loss in the range of 245–410 °C and then gradual loss up to 1000 °C, indicates the decomposition of ligand moiety. The percentage of final residue remaining above 1000 °C corresponds to the formation of thermally stable metal oxide in respective systems.

Table 1 — Elemental analyses and physical properties of NTEMNC metal complexes

Empirical formula	Yield (%)	Colour	Analyses found (calc) %				Λ_m ($\Omega^{-1}cm^2mol^{-1}$)
			C	H	N	Metal	
Cu $(C_{19}H_{16}N_5O_5)_2$. $2H_2O$	80	Parrot green	52.96 (51.38)	4.83 (4.08)	15.90 (15.77)	7.98 (7.15)	17
Ni $(C_{19}H_{16}N_5O_5)_2$. $2H_2O$	60	Yellow	53.91 (51.65)	4.79 (4.11)	15.74 (15.85)	6.84 (6.67)	15
Co $(C_{19}H_{16}N_5O_5)_2$. $2H_2O$	70	Orange	54.20 (51.66)	4.84 (4.11)	15.68 (15.85)	7.02 (6.64)	13

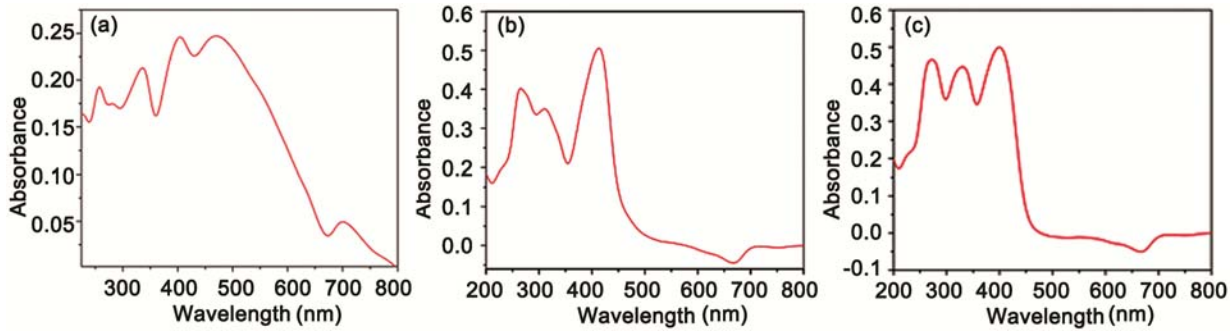

Fig. 1 — UV-vis spectrum of (a) Cu(II)-NTEMNC, (b) Ni(II)-NTEMNC, and, (c) Co(II)-NTEMNC.

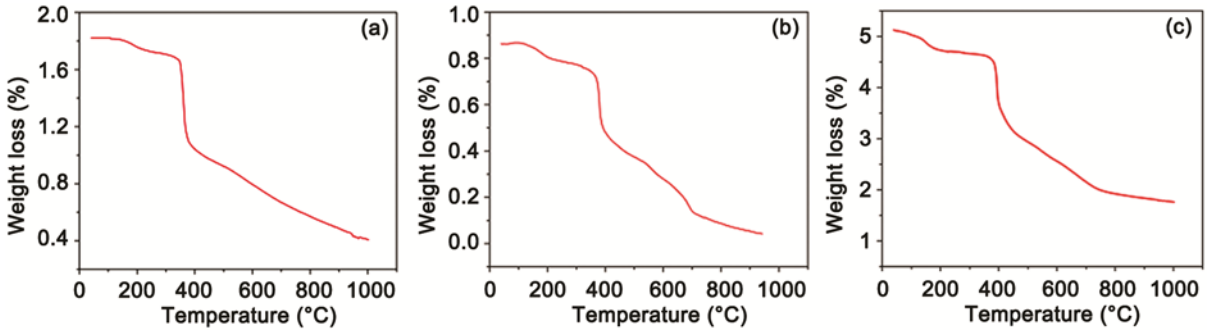

Fig. 2 — Thermogram of (a) Cu(II)-NTEMNC, (b) Co(II)-NTEMNC, and, (c) Ni(II)-NTEMNC.

ESR studies

ESR spectrum of Cu(II) complex (Fig. S14) recorded at 77 K gave $g_{\parallel}$ and $g_{\perp}$ values as 2.1196 and 2.0015 respectively. The trend $g_{\parallel} > g_{\perp}$ is characteristic for axially elongated octahedral geometry and presence of unpaired electron in $d_{x^2-y^2}$ orbital.

Magnetic susceptibilities measurements

The calculated magnetic moments of Cu(II), Ni(II) and Co(II) complexes are 1.91, 2.73 and 3.81 BM respectively. This reveals the paramagnetic behavior of all complexes, in accordance with electronic properties. A tentative structure is assigned (Fig. 3) for the metal complexes on the basis of the aforementioned results.

Molecular docking studies

Molecular docking technique is an important tool to understand the interaction of novel compounds and their metal complexes with DNA in order to understand their potential to bind at receptor sites of target nucleic acids[53]. In the present investigation, molecular docking studies of newly synthesized ligand (NTEMNC) and its Cu(II), Ni(II) and Co(II) metal complexes with DNA duplex of sequence $(AGACGTCT)_2$ (PDB ID: 1N37) were performed to predict the binding mode (Fig. 4(a)-(f)). Docking of compounds into DNA mainly showed hydrogen bonding interaction with G5 nucleotide. The molecular structure of title compounds in respective systems, is placed at larger cavity in between base pairs of target DNA helix, and then subjected to structural optimization. The optimized structure is then docked for the formation of adduct with the DNA helix. The resultant dock score and the data for type of interactions in a particular system are informative to predict the stability of docked molecule in host DNA. It has been observed that naphthyridinone group in free ligand is intercalated and consists of hydrogen bonding and π-π interactions while in Ni(II) and Cu(II)

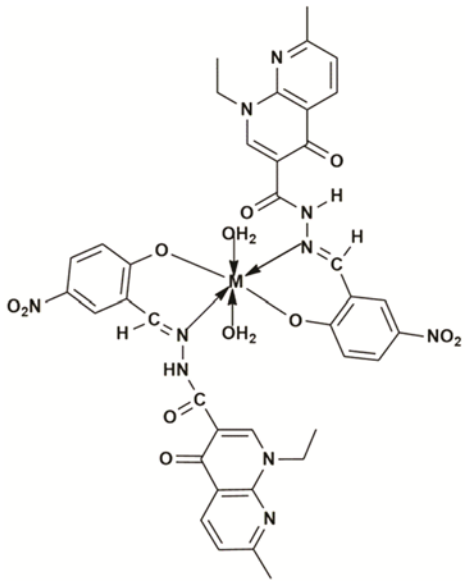

Fig. 3 — Tentative structure of complex M: Cu(II), Ni(II) and Co(II).

complexes, metal chelate part is intercalated, showing same type of interactions. The dock score provided in Table 2 represents better binding affinity of Ni(II) and Cu(II) complexes than Co(II) complex and free ligand. The inhibition constant which is high for free ligand and low for Ni(II) complex indicates lesser binding affinity with former and more binding affinity with latter. These binding affinities are in accordance to the dock score and thus the order of binding is envisaged as; Ni(II) > Cu(II) > Co(II) > NTEMNC. As the inhibition constant is very high for free ligand it can be concluded that even though there is an intercalation of moieties between base pairs of DNA, the binding affinity is far less when compared to that in complexes.

***in vitro* Biological studies**

Antimicrobial activity

The antibacterial and antifungal activity results indicate that the newly synthesized hydrazone

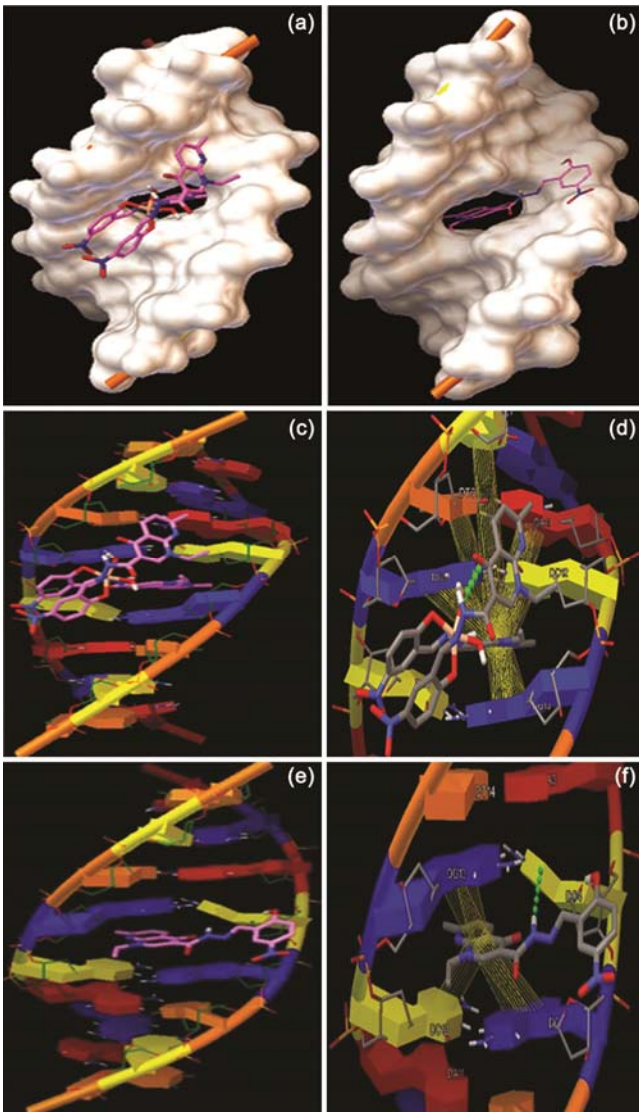

Fig. 4 — Dockpose of (a) Ni(II)-NTEMNC and (b) NTEMNC at intercalation site of DNA. Dock pose of Ni(II) complex showing hydrogen bond interaction with G5 of DNA strand and π- π stacking interaction with G5, T6, A11, C12, and G13 bases: (c) full view and (d) enlarged view. Dock pose of NTEMNC showing hydrogen bond interaction with G5 of DNA strand and π – π interaction with G5, C12 and G13 bases: (e) full view and (f) enlarged view.

(NTEMNC) and its Cu(II), Ni(II) and Co(II) complexes showed good activity against bacteria and fungi species respectively. The zone inhibition diameter (in cm) obtained against each microorganism and the relevant data are presented in Supplementary Data, Table S1 and Fig. S15. It has been observed that zone inhibition diameter increased with the increase in concentration of a test compound signifying the importance of concentration and its effect[54]. The more pronounced activity of complexes

Table 2 — Dock score and calculated inhibition constant of NTEMNC and its metal complexes

Molecule	Dock score (kcal/mol) (estimated free energy of binding)	Inhibition constant (K_i) (nM) (calculated)
NTEMNC	-5.96	42.74
Cu(II)	-8.63	0.468
Ni(II)	-9.38	0.133
Co(II)	-6.84	9.66

of NTEMNC compared to the unbound NTEMNC is because of relatively more lipophilicity of complexes which enables them to pass through the cell membrane with more ease[55]. The varying degree of inhibitory effects of different complexes on the growth of bacterial and fungal strains may be due to the effect of the respective metal ion on the cell metabolism. Interestingly, the synthesized title compound NTEMNC and its metal complexes have shown enhanced antimicrobial activity as compared to pure nalidixic acid, which is a clinically prominent antibiotic used in the treatment of urinary tract infections[56].

Cytotoxic studies

The cytotoxicity of synthesized Cu(II), Ni(II) and Co(II) metal complexes and corresponding hydrazone (NTEMNC) against HeLa (human cervical cancer cell line) and A549 (human lung tumor cell line) cell lines were evaluated by MTT assay. Experiments revealed that the cytotoxicity of the compounds was found to be concentration dependent (Fig. S16) where increase in the concentration of compounds exhibited a decrease in cell viability indicating enhanced cytotoxicity. The IC_{50} values (Table S2) for compounds reveal that the hydrazone and its complexes exhibits antitumor activity against HeLa and A549 cell lines. The microscopic images of cells after treating HeLa cell lines with compounds are presented in Fig. S17. Morphological changes are obvious in the images of cells inferring the pronounced effect of the compounds under investigation.

DNA binding studies

Absorption studies

The absorption spectra of the complexes Cu(II), Ni(II) and Co(II) in the presence and absence of CT-DNA are shown in Fig. 5. With increasing concentration of DNA, the absorption spectra of the complexes exhibited gradual decrease in absorption (hypochromism) and shift in the wavelength

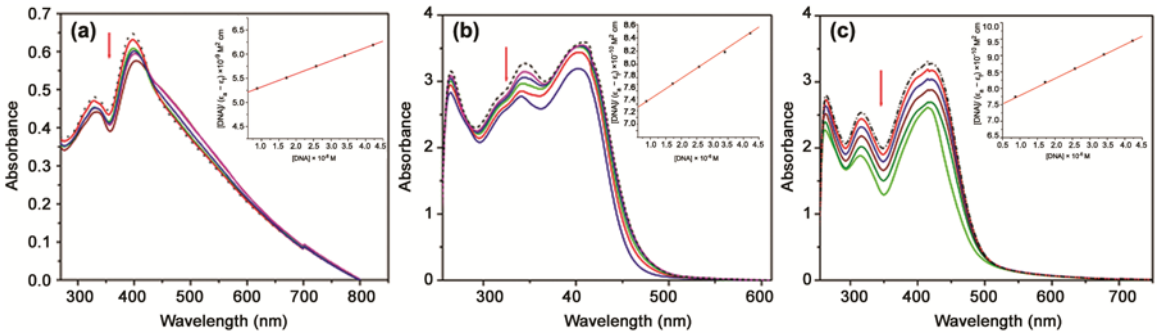

Fig. 5 — Absorption spectra of complexes (a) Cu(II), (b) Co(II), and, (c) Ni(II) in the absence (dotted line) and presence (solid line) of increasing concentration of CT-DNA in Tris-HCl buffer. Arrow (↓) shows the hypochromic and bathochromic shift upon increase of the DNA concentration [Inset: linear plot for the calculation of the intrinsic binding constant, K_b for DNA binding].

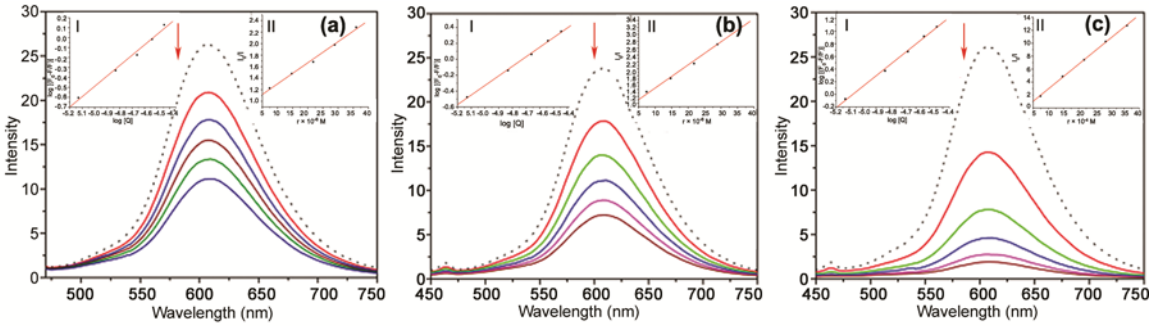

Fig. 6 — Emission spectra of the DNA-ethidium bromide (EB) with (a) Cu (II), (b) Ni(II), and, (c) Co(II), arrows show the emission intensity changes upon increasing concentration of the compounds [Inset: Scatchard equation plots (I), Stern volumer equation plots (II)].

(bathochromism/red shift), due to the intercalative mode of interaction involving a strong π-π* stacking interaction between the aromatic chromophore and the base pairs of DNA.

In order to compare quantitatively the binding strength of the complexes, the intrinsic binding constants K_b of the complexes with DNA were obtained by monitoring the changes in absorbance at 395 nm for Cu(II), 316 nm for Ni(II) and 343 nm for Co(II) with increasing concentration of DNA using the eqn (1).

Binding constant K_b is given by the ratio of slope to intercept. From the absorption data, the binding constants (K_b) for Cu(II), Co(II) and Ni(II) complexes are $5.3\pm 0.01\times10^4$ M^{-1}, $4.4\pm 0.02\times10^4$ M^{-1} and $7.0\pm0.01\times10^4$ M^{-1} respectively. These results indicate that the binding affinity of all metal complexes with CT-DNA is moderate in comparison with strong intercalators [57]. However the DNA binding affinities of these complexes follow the order: Ni(II) > Cu(II) > Co(II).

Fluorescence studies

In order to further investigate the interaction mode of Cu(II), Ni(II) and Co(II) complexes with CT-DNA, a competitive binding experiment using ethidium bromide (EB) as a probe was carried out. EB is a conjugate planar molecule with very weak fluorescence intensity due to fluorescence quenching of the free EB by solvent molecules but it is greatly enhanced when EB is specifically intercalated into the adjacent base pairs of double stranded DNA. The enhanced fluorescence can be quenched upon the addition of the second molecule which could replace the bound EB or break the secondary structure of the DNA. Upon the addition of complexes Cu(II), Ni(II) and Co(II) to CT-DNA pretreated with EB, a significant reduction in the emission intensity (Fig. 6) was observed, indicating competitive intercalation of complexes and thus effecting the equilibrium for the formation of [DNA-EB] complex. As the studied metal complexes have the potential to act as intercalators, the concentration of DNA-ethidium bromide decreases and thus results in quenching of fluorescence. The classical Stern-Volmer constant (K_{sv}), binding constant (K_b) values and number of binding sites (n) of the metal complexes are calculated using eqns (2) and (3) are in the order of Ni(II) > Cu(II) > Co(II). The K_b values estimated by

Table 3 — DNA binding studies of NTEMNC metal complexes

	CT-DNA					
	Absorption binding		Emission quenching			
Complexes	K_b	$\log K_b$	K_b	$\log K_b$	K_{sv}	n
Cu(II)	$5.3\pm 0.01\times10^4$ M^{-1}	4.72	$4.9 \pm0.02\times 10^4$ M^{-1}	4.70	$4.3\pm0.02 \times 10^4$ M^{-1}	1.20
Co(II)	$4.3\pm 0.02 \times10^4$ M^{-1}	4.63	$3.4\pm 0.02\times 10^4$ M^{-1}	4.53	$4.1\pm0.001 \times 10^4$ M^{-1}	1.04
Ni(II)	$7.0\pm0.01\times10^4$ M^{-1}	4.84	$5.3 \pm0.01\times 10^4$ M^{-1}	4.73	$8.6\pm0.001 \times 10^4$ M^{-1}	1.68

both absorption and fluorescent titrations are in good agreement (Table 3).

The docking studies discussed earlier also indicated a lower value of inhibition constant (K_i) and more negative free energy value for Ni(II) complex, suggesting its greater affinity in binding with DNA compared to other two complexes and hence one can predict that the experimental results obtained from absorption and fluorescence studies are corroborative with the predictions from computational studies.

Conclusions

Novel potential chelating agent and its binary Cu(II), Ni(II) and Co(II) metal complexes were synthesized and characterized. DNA docking studies revealed intercalative mode of binding of title ligand and its complexes involving hydrogen bonding and π- π interactions.

Absorption and fluorescence studies revealed the effective binding of title metal complexes with CT-DNA base pairs. The antitumor and antimicrobial activity of the compounds under investigation followed the order: Ni(II) > Cu(II)> Co(II) > NTEMNC.

Supplementary Data

Supplementary Data associated with this article are available in the electronic form at http://www.niscair.res.in/jinfo/ijca/IJCA_58A(04)436-445_Suppl Data.pdf.

Acknowledgement

The University Grants Commission, New Delhi, India, is gratefully acknowledged for financial support in the form of a Senior Research Fellowship to NN. The authors are grateful to UGC UPE FAR Programme. The authors thank Instrumentation Lab Facilities, Department of Chemistry and Central Facilities for Research & Development (CFRD), Osmania University. The authors acknowledge IICT Hyderabad, Sophisticated Analytical Instrument Facility (SAIF), IIT Bombay and Kalams Institute of Sciences, Hyderabad, India for the cytotoxicity studies.

References

1 Raman N, Mahalakshmi R, Arun T, Packianathan S & Rajkumar R, *J Photochem Photobiol B,* 138 (2014) 211.
2 Pyle A M & Barton J K, *Prog Inorg Chem,* 38 (1990) 413.
3 Sigman D S, *Acc Chem Res,* 19 (1986) 180.
4 Sigman D S, Mazumder A & Perrin D M, *Chem Rev*, 93 (1993) 2295.
5 Hajian R & Farkhondeh P, *Ind J Chem,* 52 A (2013) 1251.
6 Vamsikrishna N, Pradeep Kumar M, Ramesh M, Nirmal G, Sreenu D & Shivaraj, *J Chem Sci*, 129 (2017) 609.
7 Rosenberg B, VanCamp L & Krigas T, *Nature,* 205 (1965) 698.
8 Barton J K & Lolis E, *J Am Chem Soc,* 107 (1985) 708.
9 Charles D, Turner J H & Redmond C, *Bjog-Int J Obstet Gee*, 80 (2005) 264.
10 Huppert B (Ed.) *Cisplatin, Chemistry and Biochemistry of a Heading Anticancer Drug*, (Wiley VCH, Weinhein) 1999, pp. 563.
11 Guo Z & Sadler P J, *Adv Inorg Chem*, 49 (2000) 183.
12 Koiri R K, Trigun S K, Dubey S K, Singh S & Mishra L, *Biometals,* 21 (2008) 117.
13 Wu H, Kou F, Jia F, Liu B, Yuan J & Bai Y, *J Photochem Photobiol B*, 105 (2011) 190.
14 Iwasaki Y, Kimura M, Yamada A, Mutoh Y, Tateishi M, Arii H, Kitamura Y & Chikira M , *Inorg Chem Comm,* 14 (2011) 1461.
15 Tiwari A D, Mishra A K, Mishra S B, Mamba B B, Maji B & Bhattacharya S, *Spectrochim Acta, Part A,* 79 (2011) 1050.
16 Wu H L, Yuan J K, Bai Y, Pan G L, Wang H, Kong J, Fan X Y & Liu H M, *Dalton Trans*, 41 (2012) 8829.
17 Mustur C, Prabahkara, Halehatty S & Bhojya Naik, *Biometals,* 21 (2008) 675.
18 Kumar P, Baidya B, Chaturvedi S K, Khan R H, Manna D & Mondal B, *Inorg Chim Acta,* 376 (2011) 264.
19 Lippert B, *Coord Chem Rev*, 200 (2000) 487.
20 Shamsi M, Yadav S & Arjmand F, *J Photochem Photobiol B*, 136 (2014) 1.
21 Al-Mogren M M, Alaghaz A M & Ebrahem E A, *Spectrochim Acta,* 114 (2013) 695.
22 Arjmand F, Muddassir M & Khan R H, *Eur J Med Chem*, 45 (2010) 3549.
23 Richards A D & Rodger A, *Chem Soc Rev,* 36 (2007) 471.
24 Terron A, Fiol J J, García Raso A, Barceló Oliver M & Moreno V, *Coord Chem Rev*, 251 (2007) 1973.
25 Keene F R, Smith J A & Collins J G, *Coord Chem Rev*, 253 (2009) 2021.
26 Zeglis B M, Pierre V C & Barton J K, *Chem Comm,* 44 (2007) 4565.
27 Arjmand F, Jamsheera A & Mohapatra D K, *J Photochem Photobiol B*, 121 (2013) 75.

28 Erkkila K E, Odom D T & Barton J K, *Chem Rev,* 99 (1999) 2777.

29 Liu Z C, Wang B D, Li B, Wang Q, Yang Z Y, Li T R & Li Y, *Eur J Med Chem*, 45 (2010) 5353.

30 Ramakrishnan S, Shakthipriya D, Suresh E, Periasamy V S, Akbarsha M A & Palaniandavar M, *Inorg Chem*, 50 (2016) 458.

31 Justin Dhanaraj C, Hassan I U, Johnson J, Joseph J & Selwin Joseyphus R, *J Photochem Photobiol B*, 162 (2016) 115.

32 Joseph J, Nagashri K & Suman A, *J Photochem Photobiol B*, 162 (2016) 125.

33 Justin Dhanaraj C & Johnson J, *Spectro chimica Acta*, 118 (2014) 624.

34 Ansari I A, Sama F, Raizada M, Shahid M, Rajpoot R K & Siddiqi Z A, *J Mol Struct*,1127 (2017) 479.

35 Sivasankaran Nair M, Arish D & Johnson J, *J Saudi Chem Soci,* 20 (2016) 591.

36 Narsimha N, Ranjith reddy P, Jaheer M D, Aparna B & Sarala Devi C H, *Int J Res Pharm Chem*, 5 (2015) 615.

37 Narsimha N, Sudeepa K, Jaheer M D, Ravi M, Sreekanth S & Sarala Devi C H, *J Fluor,* 28 (2017) 225.

38 Jaheer M D, Ranjith Reddy P, Aparna B, Shravan Kumar G & Sarala devi C H, *Int J Pharma Sci Rev Res,* 35 (2015) 84.

39 Searle M S, Maynard A J & Williams H E, *Org Biomol Chem,* 1 (2003) 6.

40 Scanner M F, *J Mol Graph Model*, 17 (1999) 57.

41 Ravi M, Kishan Prasad C H, Ushaiah B, Ravi Kumar E, Shyam P & Sarala Devi C H, *J Fluoresc*, 25 (2015) 1279.

42 Rambabu A, Pradeep Kumar M, Tejaswi S, Vamsikrishna V & Shivaraj, *J Photochem Photobiol B*, 165 (2016) 147.

43 Kishan Prasad C H, Ravi M, Ushaiah B, Srinu V, Ravi Kumar E & Sarala Devi C H, *J Fluoresc,* 26 (2016) 189.

44 Wang Q, Mao H, Wang W, Zhu H, Dai L, Chen Y & Tang X, *Biometals,* 30 (2017) 575.

45 Sudeepa K, Narsimha N, Aparna B, Sreekanth S, Aparna A V, Ravi M, Jaheer M D & Sarala devi C H, *J Chem Sci,* 130 (2018) 52.

46 Deepika N, Praveen Kumar Y, Shobha Devi C, Venkat Reddy P, Srishailam A & Satyanarayana S, *J Biolog Inor Chem,* 18 (2013) 751.

47 Srishailam A, Gabra N, Praveen Kumar Y, Laxma Reddy K, Shobha Devi C, Anil Kumar D, Singh S S & Satyanarayana S, *J Photochem Photobiol B*, 141 (2014) 47.

48 Bellamy L J, *The infra-red spectra of complex molecules*, 2nd edn, (London) 1958.

49 Nakamoto K, *Infrared Spectra of Inorganic and Coordination Compounds, Part B*, 5th edn, (Wiley Interscience, New York) 1971.

50 Sudeepa K, Aparna B, Ravi M, Ranjith Reddy P, Karunakar Rao K & Sarala Devi C H, *Int J Res Pharm Chem*, 5 (2015) 668.

51 Nakamoto K, *Infrared and Raman Spectra of Inorganic and Coordination Compounds*, 5th edn, (Wiley-Interscience, New York) 1997.

52 Bellamy L J, *The Infrared Spectra of Complex Molecules*, *Second Ed*, (London) 1980.

53 Justin Dhanaraj C, Hassan I U, Johnsona J, Joseph J & Selwin Joseyphus R, *J Photochem Photobiol B*, 162 (2016) 115.

54 Shobha Devi C, Anil Kumar D, Singh S S, Gabra N, Deepika N, Praveen Kumar Y & Satyanarayana S, *Eur J Med Chem*, 64 (2013) 410.

55 Reddy P N, Nethaji M & Chakravarthy A R, *Eur J Inorg Chem*, 7 (2004) 1440.

56 Emmerson A M & Jones A M, *J Antimicro Chemo*, 51 (2003) 13.

57 Rabindra Reddy P, Rajeshwar S & Satyanarayan B, *J Photochem Photobiol B*, 160 (2016) 217.